

Article

Theoretical Study of Adsorption of Group IIIA Nitrides on Si(111)

Demeter Tzeli, Ioannis D. Petsalakis, and Giannoula Theodorakopoulos

J. Phys. Chem. C, **2009**, 113 (14), 5563-5567 • Publication Date (Web): 16 March 2009

Downloaded from <http://pubs.acs.org> on April 2, 2009

More About This Article

Additional resources and features associated with this article are available within the HTML version:

- Supporting Information
- Access to high resolution figures
- Links to articles and content related to this article
- Copyright permission to reproduce figures and/or text from this article

[View the Full Text HTML](#)

Theoretical Study of Adsorption of Group IIIA Nitrides on Si(111)

Demeter Tzeli,* Ioannis D. Petsalakis, and Giannoula Theodorakopoulos

Theoretical and Physical Chemistry Institute, National Hellenic Research Foundation,
48 Vassileos Constantinou Avenue, Athens 116 35, Greece

Received: December 9, 2008; Revised Manuscript Received: January 20, 2009

Adsorption of group IIIA nitrides (MN, M = B, Al, Ga, and In) on a model Si(111) surface has been studied by density functional theory calculations. Eight stable structures were determined for the MN adsorbed species. Their lowest energy structures are those with the adsorbate forming a bridge between the Si adatom and the Si rest atom as well as open structures with the M–N molecule attached to a Si adatom or a Si rest atom via N. The energy ordering of these stable structures varies according to the particular metal atom. The binding energy, including the basis set superposition error, of the lowest calculated minimum MN–Si(111) structure for the different metals M ranges from 5.1 to 6.0 eV.

I. Introduction

The study of chemisorption of group IIIA metals and their nitrides at Si surfaces presents great interest because the group IIIA nitrides are very promising optoelectronic materials for many applications such as light-emitting diodes, laser diodes, and high-power and high-temperature electronic devices.^{1,2} Moreover, silicon is very interesting as a substrate because of the favorable physical properties, high quality, very low cost, and mature development for processing and large-scale production.³ The epitaxial growth of group IIIA nitrides on Si surfaces is a promising route for large-scale, low-cost mass production of group IIIA nitride-based devices.⁴ All the above make the study of group IIIA nitrides at Si surfaces very interesting and potentially useful. Subjects of particular interest are the geometric and electronic structure of chemisorbed group IIIA nitrides and the growth of their films on Si surface, BN,^{5,6} AlN,^{4,5,7} GaN,^{3–5,8–14} and InN.^{15–17}

Even though there are many experimental studies of group IIIA nitrides^{4,7–17} deposited on Si(111) and mainly on the growth of their films on Si(111) surface, theoretical studies have been almost entirely devoted to the adsorption of group IIIA metal atoms (B, Al, Ga, In) on Si(111) (see, for instance, refs 18–22 and references therein), while recently work was published by the present authors on Ga as well as on gallium nitrides adsorbed on Si(111).^{23,24}

The present study is a continuation of our previous study^{23,24} of the electronic and geometric chemisorbed structures of gallium (Ga, Ga⁺) and gallium nitrides (GaN, GaN⁺, GaN₂, GaN₂⁺) on Si(111) using density functional theory (DFT) calculations and a Si₂₆H₂₂ model of the Si(111) surface. It is important to extend the study to other group IIIA metal nitrides, since they all are technologically important to varying degrees, while there are differences in the different metal atoms, such as size and electronegativity, which will conceivably lead to differences in the mode of adsorption at the Si surface. In the present work, the study is expanded to include adsorption at Si(111) of other group IIIA nitrides, while some additional low-lying minimum energy structures have been determined for adsorbed GaN. Thus, the electronic and geometric chemisorbed

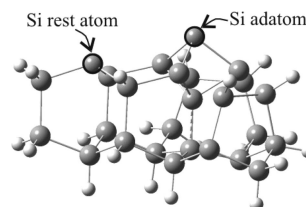


Figure 1. Five-layer one-rest one-adatom (1R-1A) cluster model of Si(111) (Si, gray spheres; H, white spheres).

structures of BN, AlN, GaN, and InN at Si(111) employing the same methodology as previously used²³ are determined.

II. Computational Procedure

The chemisorbed structures of MN, M = B, Al, Ga, and In, at Si(111) are calculated at a five-layer one-rest one-adatom (1R-1A) cluster model of Si(111), see Figure 1, constructed as previously described^{23,25} using the dimer-adatom-stacking fault (DAS) structure²⁶ and the low-energy electron diffraction (LEED) data of Tong et al.²⁷ for the Si(111) reconstructed surface. Hydrogen atoms (white spheres) have been added to terminate the 26-Si atom cluster (gray spheres, Si) at the sides as well as below the lowest Si level (cf. Figure 1), while the adatom and the rest atom are left with one dangling bond (i.e., one unpaired electron) each.

DFT calculations were carried out using the B3LYP functional^{28,29} and the DGDZVP basis set (double- ζ valence plus polarization, i.e., [3s2p1d_{B,N}/4s3p1d_{Al,Si}/5s4p2d_{Ga}/6s5p3d_{In}]).³⁰ This combination was considered to be the best choice for the present calculations (see also ref 23) since the large size (50 atoms) of the systems calculated practically forbids the use of multi reference configuration interaction (MRCI) or coupled cluster (CC) methods. On the other hand, the B3LYP/DGDZVP calculations on the diatomic molecules MN, MSi, and NSi show satisfactory similarity with the best known ab initio calculations and experiment; compare Table 1, where some results on the above diatomic systems are given. For some of the systems of Table 1, additional tests have been carried out previously using different kinds of basis sets such as LANL2DZ, 6–31+G, 6–31G(d), 6–311+G(2df), and DGDZVP and functionals such as B3LYP, B3PW91, BPBEPBE, and LSDA.²⁴

* To whom correspondence should be addressed. Fax: +30-210-7273-794; e-mail: dtzeli@eie.gr.

TABLE 1: Geometries R_e (Å), Dissociation Energies D_e (eV), Harmonic Frequencies ω_e (cm⁻¹), Dipole Moments μ (Debye), and Mulliken Charges q_x^a of the BN, AlN, GaN, InN, BSi, AlSi, GaSi, InSi, and SiN Molecules

molecule	method	R_e (Å)	D_e (eV)	ω_e	μ	q_x
BN($X^3\Pi$)	B3LYP/LANL2DZ	1.359	3.95	1449	1.90	+0.64
	B3LYP/DGDZVP	1.329	4.66	1557	2.00	+0.68
	MRCI/cc-pVQZ ³⁷	1.330	4.43	1515	1.95	+0.28
	expt	1.329 ³⁸	3.99 ± 0.5 ^b 39	1519.2 ⁴⁰		
AlN($X^3\Pi$)	B3LYP/LANL2DZ	1.863	2.13	664.1	2.66	+0.78
	B3LYP/DGDZVP	1.811	2.56	725.3	2.73	+0.84
	MRCI+DKH2+Q/cc-pV5Z ⁴¹	1.797	2.52	751.0	2.71	+0.34
	expt	1.7864 ⁴²	2.9 ± 0.4 ⁴³	758.4 ⁴²		
GaN($X^3\Sigma^-$)	B3LYP/LANL2DZ	2.067	1.97	449.1	2.43	+0.67
	B3LYP/DGDZVP	2.046	2.17	472.6	2.16	+0.66
	RCCSD(T)/aug-cc-pV5Z(-PP) ³⁴	2.041	2.05			
	CBS-RCCSD(T)/cc-p(wC)VnZ(-PP) ³⁴	1.985	2.12			
InN($X^3\Sigma^-$)	B3LYP/LANL2DZ	2.240	1.77	403.7	2.89	+0.69
	CCSD(T)/ANO-RCC ⁴⁴	2.206	1.77	445.5	3.32	
	A ³ Π	B3LYP/LANL2DZ	2.061	1.68	482.0	3.06
BSi($X^4\Sigma^-$)	B3LYP/DGDZVP	2.115	1.67	476.3	3.37	+0.75
	CCSD(T)/ANO-RCC ⁴⁴	2.064	1.65	517.4	2.61	
	B3LYP/LANL2DZ	1.956	2.95	691.1	0.28	-0.18
	B3LYP/DGDZVP	1.926	3.18	734.6	0.59	-0.19
AlSi($X^4\Sigma^-$)	QCISD(T)/6-311+G(2df)//MP2(full) ⁴⁵	1.905	3.15	772		
	expt ⁴⁶		2.95 ^b			
	B3LYP/LANL2DZ	2.514	2.16	333.3	1.80	+0.36
	B3LYP/DGDZVP	2.451	2.29	354.6	1.55	+0.35
GaSi($X^4\Sigma^-$)	MRCI/cc-pVQZ ⁴⁷	2.424	2.53	385	1.27	
	expt ⁴⁶		2.34 ^b			
	B3LYP/LANL2DZ	2.525	2.12	266.7	1.92	+0.34
	B3LYP/DGDZVP	2.457	2.24	282.1	1.42	+0.29
InSi($X^4\Sigma^-$)	MRCI/cc-p(wC)VQZ(-PP) ⁴⁸	2.406	2.38			
	B3LYP/LANL2DZ	2.699	2.01	234.1	2.54	+0.43
	B3LYP/DGDZVP	2.660	2.09	253.3	1.95	+0.39
	MRCI/cc-p(wC)VQZ(-PP) ⁴⁸	2.601	2.19			
SiN($X^2\Sigma^+$)	B3LYP/LANL2DZ	1.606	3.70	1094	2.47	+0.90
	B3LYP/DGDZVP	1.579	4.43	1169	2.69	+0.97
	CIQ/STO-(8s6p3d2f) ⁴⁹	1.568	3.84	1177		
	expt ⁵⁰	1.572		1138 ^c		

^a X = the first atom of the molecule. ^b D_0^0 value. ^c $\Delta G_{1/2}$.

As shown in Table 1, the differences in R_e of DFT(B3LYP/DGDZVP) and the best ab initio calculation or experiment range from 0.001 (BN) to 0.06 Å (InSi) while the differences in dissociation energy of DFT and the best ab initio calculation or experiment range from 0 (InN) to 0.2 eV (BN). In addition to the calculations employing B3LYP/DGDZVP, calculations employing the Hay–Wadt LANL2DZ ECP³¹ basis sets were carried out in an effort to account for the relativistic effects, which might be of importance for Ga and In. These basis sets consist of a pseudopotential for the core electrons, up to 3d(4d) electrons of Ga(In), up to 2p electrons of Si and Al, and a double- ζ quality basis set for the three outer electrons of Ga(In) 4s²4p¹(5s²5p¹), for the three(four) outer electrons of Al(Si), and for the five(seven) electrons of B(N), that is, (3s3p)→[2s2p]_{Ga,In}, (3s3p)→[2s2p]_{Al,Si}, and (10s5p)→[3s2p]_{B,N}.

Employing both the B3LYP/DGDZVP and the B3LYP/LANL2DZ techniques, the electronic and geometric structures of chemisorbed group IIIA nitrides (MN, M = B, Al, Ga, and In) on the five-layer 1R-1A cluster of Si (see Figure 1) were investigated. Eight chemisorbed structures for each of MN–Si(111) were determined by energy optimization with respect to the coordinates of the Si rest and the Si adatom as well as those of the adsorbed species in each case. The remaining cluster was kept fixed to retain the Si(111) surface structure.

For all stable geometries, binding energy (BE) of each species to the surface was calculated, where the basis set superposition error (BSSE) was estimated with respect to the relevant fragments by the counterpoise procedure^{32,33} for the sake of

completeness. The BSSE must be taken into account when the bonding is weak; however, it is not uncommon in cases with large BE that the BSSE needs to be taken into account; see, for instance, ref 34. All calculations were performed using the Gaussian 03 program package.³⁵

III. Results

The structures which were determined for the MN–Si(111) cluster are given in Figure 2, M = B, Al, Ga, and In. In what follows, the minima are labeled by the geometric structure, **a–h** (cf. Figure 2), followed by the name of the adsorbed species, for example, **a**-BN stands for the minimum corresponding to the **a** structure of Figure 2 for the BN–Si(111) cluster. The MN–Si(111) structures are calculated having singlet, triplet, and quintet multiplicity. For all MN–Si(111) structures, the triplets are the lowest minima, and for brevity, only the lowest energy structures of triplet multiplicity are presented here.

The optimum geometries, the binding energies, and the natural population analysis (npa) of the structures determined are given in Table 2 for MN–Si(111) at the B3LYP/DGDZVP level of theory as well as the binding energies at the B3LYP/LANL2DZ level. Generally, there are no significant differences in geometry (R , ϕ of Figure 2) and npa between the B3LYP/DGDZVP and the B3LYP/LANL2DZ calculations. In a few structures, where the MN molecule (M = Al, Ga, and In) forms a bridge between the Si rest and the Si adatom, the largest differences for the calculated R values by the two levels of calculation reach 0.1

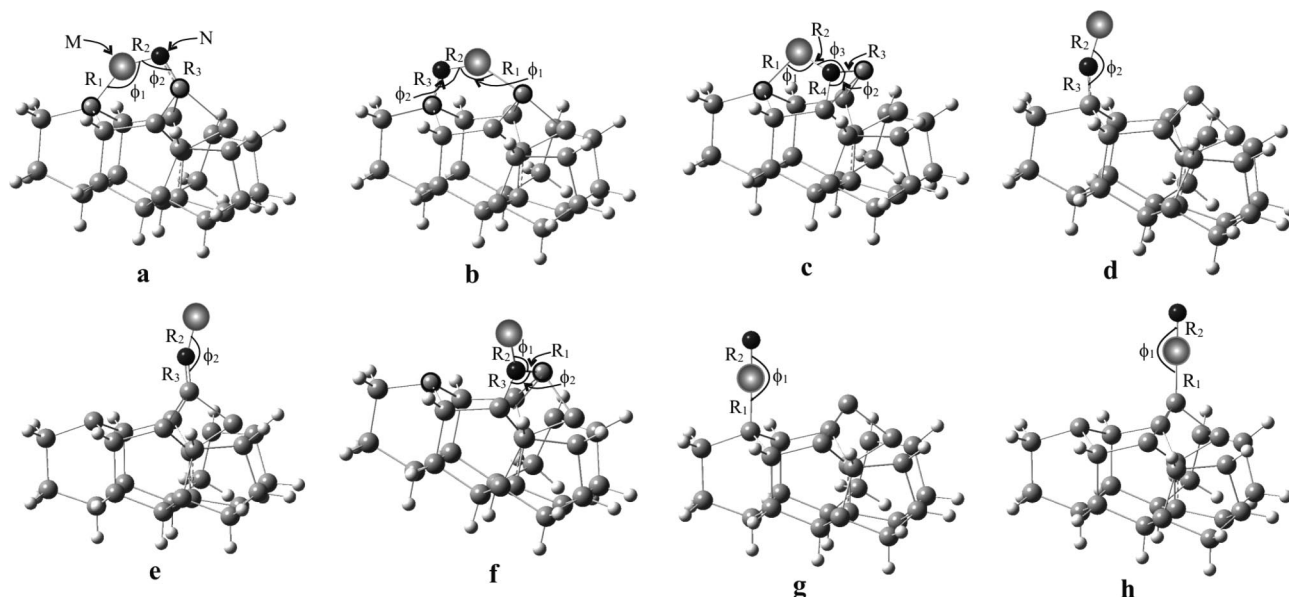


Figure 2. Eight structures of MN–Si(111), M = B, Al, Ga, and In.

TABLE 2: Geometry R (Å), ϕ (degrees), Binding Energies BE (eV), and Corrected Values for BSSE BE_{BSSE} (eV) and Net Charges of the MN–Si(111) Structures, M = B, Al, Ga, and In, at B3LYP/DGDZVP Level of Theory

structure	R_1	R_2	R_3	R_4	ϕ_1	ϕ_2	ϕ_3	Si rest	Si adat	M	N	BE (BE _{BSSE})	BE (BE _{BSSE}) ^a
BN–Si(111)													
a-BN	2.01	1.29	1.77		145	123		−0.04	+0.81	+0.62	−1.33	6.09(5.96)	6.14(5.82)
b-BN	2.04	1.29	1.77		145	127		+0.67	+0.10	+0.58	−1.34	6.02(5.85)	6.00(5.69)
d-BN		1.26	1.73			178		+0.64	+0.19	+0.85	−1.44	4.86(4.75)	4.94(4.70)
e-BN		1.26	1.72			179		+0.10	+0.80	+0.61	−1.54	4.73(4.61)	4.76(4.53)
f-BN	1.83	1.37	1.80		122	113		+0.09	+0.77	+0.56	−1.80	4.67(4.58)	4.73(4.49)
g-BN	1.96	1.30			172			−0.05	+0.29	+0.31	−0.73	3.98(3.90)	4.12(3.86)
h-BN	1.96	1.31			179			+0.10	+0.14	+0.22	−0.70	3.67(3.60)	3.82(3.62)
AlN–Si(111)													
a-AlN	2.49	1.72	1.72		142	108		−0.42	+0.87	+1.51	−1.75	4.58(4.46)	4.22(4.20)
b-AlN	2.50	1.73	1.72		131	124		+0.77	−0.26	+1.37	−1.78	4.76(4.53)	4.24(3.49)
c-AlN	2.72	1.88	1.80	1.77	109	109	113	−0.35	+0.78	+1.14	−1.96	5.39(5.27)	
d-AlN		1.82	1.69		177			+0.75	+0.15	+0.77	−1.59	4.11(4.03)	3.83(3.20)
e-AlN		1.77	1.66		157			+0.09	+0.93	+0.92	−1.75	4.17(4.09)	3.96(3.66)
f-AlN	1.78	1.85	1.78		122	109		+0.07	+0.84	+0.88	−2.05	4.95(4.84)	5.37(5.15)
g-AlN	2.45	1.75			178			−0.50	+0.20	+1.32	−1.00	1.89(1.81)	1.88(1.79)
h-AlN	2.46	1.76			179			+0.08	−0.40	+1.30	−1.00	1.67(1.59)	1.68(1.60)
GaN–Si(111)													
a-GaN	2.47	1.77	1.73		143	106		−0.30	+0.86	+1.27	−1.63	4.10(3.95)	3.92(3.54)
b-GaN	2.50	1.78	1.73		133	119		+0.75	−0.16	+1.14	−1.65	4.32(4.23)	3.96(3.23)
c-GaN	2.93	2.25	1.69	1.79	96	97	121	−0.43	+1.08	+0.73	−1.83	4.98(4.72)	
d-GaN		1.89	1.70			161		+0.73	+0.22	+0.77	−1.46	3.93(3.84)	3.89(3.76)
e-GaN		1.85	1.63			159		+0.09	+0.96	+0.78	−1.71	3.79(3.70)	3.86(3.74)
f-GaN	1.77	1.94	1.77		123	109		+0.07	+0.80	+0.83	−2.00	5.26(5.14)	5.28(4.99)
g-GaN	2.40	1.78			179			−0.39	+0.18	+1.10	−0.89	1.72(1.62)	1.69(1.57)
h-GaN	2.41	1.78			179			+0.09	−0.21	+0.97	−0.68	1.50(1.41)	1.60(1.49)
InN–Si(111)													
a-InN	2.84	2.12	1.69		110	120		−0.36	+0.87	+1.06	−1.50	4.04(3.89)	3.46(3.21)
b-InN	2.71	2.03	1.72		127	116		+0.74	−0.21	+1.23	−1.63	4.23(4.22)	3.49(2.77)
c-InN	2.98	2.50	1.68	1.78	91	97	115	−0.51	+1.08	+0.76	−1.79	5.45(5.17)	
d-InN		2.14	1.70			169		+0.69	+0.15	+0.80	−1.42	3.86(3.78)	3.75(3.49)
e-InN		2.12	1.66			174		+0.08	+0.85	+0.80	−1.51	4.09(4.02)	3.77(3.56)
f-InN	1.76	2.18	1.76		119	111		+0.06	+0.71	+0.87	−2.00	5.44(5.31)	5.11(4.83)
g-InN	2.62	2.01			178			−0.47	+0.18	+1.21	−0.88	1.45(1.35)	1.09(0.92)
h-InN	2.62	2.01			180			+0.08	−0.38	+1.20	−0.90	1.25(1.13)	1.09(0.96)

^a B3LYP/LANL2DZ.

Å, while for a-AlN and a-GaN, there is a difference of up to 50 degrees for the ϕ_1 and ϕ_2 angles, and for a-InN, there is a difference of up to 23 degrees for the ϕ_1 and ϕ_2 angles. The reason for these discrepancies is that the B3LYP/DGDZVP and

the B3LYP/LANL2DZ methods have resulted in a slightly different conformation of bridged structures as the lowest a structure. In Table 1, only the B3LYP/DGDZVP geometry and npa are given, which we consider as our best results. For the

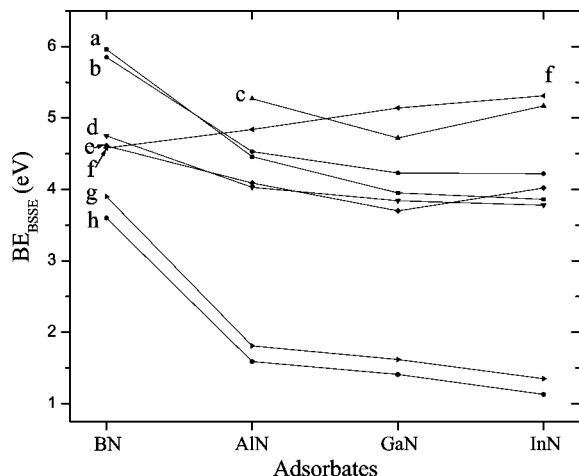


Figure 3. The BSSE corrected binding energies BE_{BSSE} of the minima (a–h) with respect to the MN adsorbates at B3LYP/DGDZVP level of theory.

BE, the B3LYP/LANL2DZ values refer to the optimum structure obtained at this level.

Eight local minima (a–h, cf. Figure 2) have been determined for adsorbed MN, where in a–c MN forms a bridge between the Si adatom and the Si rest atom, and especially in c, the N atom is directly above a second-layer Si atom adjacent to the adatom. In the d and e structures, the MN molecule is normal to the surface with the N atom attached to the Si rest atom and to the Si adatom, respectively. At the f minimum, the MN molecule is again aligned perpendicularly and the N atom is connected to the Si adatom at an angle so that it is almost directly above a second-layer Si atom adjacent to the adatom. In the last two structures, g and h, MN is also normal to the surface but with M connected to the Si rest atom and the Si adatom, respectively.

The geometry and the binding energy of the MN–Si(111) cluster and the npa of the adsorbed MN and of the Si adatom and Si rest atom are given in Table 2. Graphically, the BE_{BSSE} values of the eight minima with respect to the MN adsorbates are given in Figure 3.

As can be seen from Table 2, the structures of AlN–Si(111) and GaN–Si(111) have similar geometries. Moreover, the BN adsorbates have the shortest R_{M-Si} distances in all structures by about 0.5 Å compared to the R_{M-Si} distances of the AlN and GaN adsorbates and by 0.7 Å compared to the R_{M-Si} values of InN. Similar differences are found between the corresponding R_{M-Si} values of the ground states of the diatomic MSi molecules; compare Tables 1 and 2.

We observe that the adsorbed BN species present the largest BE_{BSSE} for all structures with the exception of structure f. The a minimum is the lowest of the BN adsorbed species with $BE_{BSSE} = 5.96$ eV, while the b minimum is very close with $BE_{BSSE} = 5.85$ eV. The c structure for BN is unstable because of the geometry requirements of this structure and the small size of the B atom; optimization of its geometry leads to the a minimum. The two lowest minima of AlN–Si(111) are the c and f structures, and their binding energies are 5.27 and 4.84 eV, respectively. The next two adsorbates, GaN and InN, have the f minimum as the lowest with $BE = 5.14$ (GaN) and 5.31 eV (InN), while their next lowest minimum is of the c structure with $BE = 4.72$ (GaN) and 5.17 eV (InN). Thus, for the lowest minimum of all four MN adsorbates, the BE ranges from 5.14 to 5.96 eV. Even though the AlN–Si(111) and GaN–Si(111) clusters have practically the same geometries in all structures,

the AlN adsorbates have larger BE than the corresponding values of the GaN adsorbates by 0.18–0.55 eV with the exception of the f structure, where the GaN adsorbate has larger BE by 0.30 eV than the corresponding structure of the AlN adsorbate (cf. Table 2). Moreover, the two AlN and GaN adsorbates have different lowest calculated MN–Si(111) minima, the c and f structures, respectively. This work is a continuation of our previous studies^{23,24} not only because it is expanded to include adsorption at Si(111) of other group IIIA nitrides (BN, AlN, and InN) but also because additional low-lying minimum energy structures were checked as possible minima. Structures c and f for adsorbed GaN turned out to be lower minima by 0.9 and 0.5 eV than the b structure which had been found to be the lowest calculated minimum in our previous studies.^{23,24}

The variation of the BE of the different structures a–h with the M atomic number is shown in Figure 3. For four structures out of the eight, that is, a, b, g, and h, as the M atomic number increases the BE_{BSSE} of each structure decreases, while for the f minimum, the BE_{BSSE} of each structure increases with the atomic number. This may be rationalized in terms of the details of the bonding geometry in each structure, where the size of the metal atom may hinder or facilitate the bonding. For structures c–e, the variation in BE with M is small because only the N atom is connected to the surface. Moreover, for each of the eight structures of MN–Si(111), M = Al, Ga, and In (excluding B), the BEs are similar with the largest difference being 0.55 eV. Finally, the energy ordering of the stable structures varies with the particular metal atom: a, b, d, e, f, g, h for BN; c, f, b, a, e, d, g, h for AlN; f, c, b, a, d, e, g, h for GaN; and f, c, b, e, a, d, g, h for InN.

There is no significant difference in the BE_{BSSE} calculated at B3LYP/DGDZVP and B3LYP/LANL2DZ levels for most of the structures with some exceptions for the AlN, GaN, and InN adsorbates as in the case of their b structures and d–AlN structure where the differences of the BSSE corrected values range from 0.8 and 1.4 eV (cf. Table 2). However, the differences of the above uncorrected BE for the BSSE vary a lot less, ranging from 0.4 to 0.7 eV, showing that the reason for these big differences is the large calculated BSSE for the B3LYP/LANL2DZ level which in these cases underestimates the BE. For the c structures of the AlN, GaN, and InN adsorbates, the geometry optimization failed at the B3LYP/LANL2DZ level of theory because calculations did not converge.

Finally, the npa shows that the surface acts as a pool of electronic charge for the MN molecules, and there is a transfer of electronic charge from the surface to MN in most structures calculated (cf. Table 2). In all minima of adsorbed MN, the partial charges on M = Al, Ga, and In range from +0.73 and +1.51 and on B range from +0.22 to +0.85 (cf. Table 2). However, the partial charges at N are negative with the resulting net charges for adsorbed MN, M = Al, Ga, and In, ranging from –0.24 to –1.24 with the exception of the g and h structures of MN–Si(111) where the MN has a positive charge of about 0.3 e^- . Both basis sets give similar charges on the different atoms.

IV. Conclusions

The electronic and geometric structures of group IIIA nitrides (MN) adsorbed on Si(111), M = B, Al, Ga, and In, were studied by DFT calculations and a five-layer, one rest atom, and one adatom Si cluster model of the Si(111) surface terminated with H atoms. Eight stable structures were determined for the MN adsorbed species of which three are bridged structures with the adsorbate bridging between the Si rest atom and Si adatom and

five are open structures with the MN molecule attached to a Si adatom or a Si rest atom. The energy ordering of these stable structures varies according to the particular metal atom. The adsorbed BN structure has the largest BE_{BSSE} (binding energy corrected for the basis set superposition error) and the shortest R_{M-Si} distances among the MN adsorbates. The BE_{BSSE} values of the lowest calculated MN–Si(111) minima are 5.96 (BN), 5.27 (AlN), 5.14 (GaN), and 5.31 (InN) eV at the B3LYP/DGDZVP level of theory.

Given the limitations of the DFT methodology, there could be some uncertainty in the above values but in no case larger than 10% which is a common value for most DFT calculations.³⁶ However, the gross features of the energy ordering of the structures and the trends will not be washed out except for cases with energy differences less than 0.1 eV, where some changes might occur. On the other hand, for the geometry, we estimate the uncertainty to be around 2%.

Acknowledgment. Financial support from the EU FP7, Capacities Program, NANOHOST project (GA 201729) is acknowledged.

References and Notes

- (1) Nakamura, S. *Science* **1998**, *281*, 956.
- (2) Taniyasu, Y.; Kasu, M.; Makimoto, T. *Nature* **2006**, *441*, 7091.
- (3) Liu, X. Y.; Li, H. F.; Uddin, A.; Andersson, T. G. *J. Cryst. Growth* **2007**, *300*, 114.
- (4) Vézian, S.; Le Louarn, A.; Massies, J. *J. Cryst. Growth* **2007**, *303*, 419.
- (5) Davis, R. F.; Paisley, M. J.; Sitar, Z.; Kester, D. J.; Ailey, K. S.; Linthicum, K.; Rowland, L. B.; Tanaka, S.; Kern, R. S. *J. Cryst. Growth* **1997**, *178*, 87.
- (6) Zhou, H.; Wang, R. Z.; Huang, A. P.; Wang, M.; Wang, H.; Wang, B.; Yan, H. *J. Cryst. Growth* **2002**, *241*, 261.
- (7) Meng, G.; Liu, X.; Xie, S.; Peng, D. *J. Cryst. Growth* **1996**, *163*, 232.
- (8) Yang, Y.-G.; Ma, H.-L.; Xue, C.-S.; Hao, X.-T.; Zhuang, H.-Z.; Ma, J. *Physica B* **2003**, *325*, 230.
- (9) Xue, C.; Yang, L.; Wang, C.; Zhuang, H.; Wei, Q. *Appl. Surf. Sci.* **2003**, *210*, 153.
- (10) Dadgar, A.; Schulze, F.; Wienecke, M.; Gadanez, A.; Bläsing, J.; Veit, P.; Hempel, T.; Diez, A.; Christen, J.; Krost, A. *New J. Phys.* **2007**, *9*, 389.
- (11) Takemoto, K.; Murakami, H.; Iwamoto, T.; Matsuo, Y.; Kangawa, Y.; Kumagai, Y.; Koukitu, A. *Jpn. J. Appl. Phys.* **2006**, *45*, L478.
- (12) Naritsuka, S.; Kondo, T.; Otsubo, H.; Saitoh, K.; Yamamoto, Y.; Maruyama, T. *J. Cryst. Growth* **2007**, *300*, 118.
- (13) Ishikawa, H.; Yamamoto, K.; Egawa, T.; Soga, T.; Jimbo, T.; Umeno, M. *J. Cryst. Growth* **1998**, *189/190*, 178.
- (14) Wu, Y.; Xue, C.; Zhuang, H.; Tian, D.; Liu, Y.; He, J.; Wang, F.; Sun, L.; Ai, Y. *Mater. Lett.* **2006**, *60*, 3076.
- (15) Ji, X. H.; Lau, S. P.; Yang, H. J.; Zhang, Q. Y. *Thin Solid Films* **2007**, *515*, 4619.
- (16) Chang, K. J.; Chang, J. Y.; Chen, M. C.; Lahn, S. M.; Kao, C. J.; Li, Z. Y.; Uen, W. Y.; Chi, G. C. *J. Vac. Sci. Technol.* **2007**, *25*, 701.
- (17) Yodo, T.; Shimada, T.; Tagawa, S.; Harada, Y. *J. Cryst. Growth* **2007**, *301–302*, 504.
- (18) Lyo, I.-W.; Kaxiras, E.; Avouris, P. *Phys. Rev. Lett.* **1989**, *63*, 1261.
- (19) Wang, S.; Radny, M. W.; Smith, P. V. *J. Phys.: Condens. Matter* **1997**, *9*, 4535.
- (20) Hoshino, T.; Okano, K.; Enomoto, N.; Hata, M.; Tsuda, M. *Surf. Sci.* **1999**, *423*, 117.
- (21) Cho, K. N.; Kaxiras, E. *Surf. Sci.* **1998**, *396*, L261.
- (22) Tzeli, D.; Petsalakis, I. D.; Theodorakopoulos, G. To be submitted.
- (23) Tzeli, D.; Petsalakis, I. D.; Theodorakopoulos, G. *Chem. Phys. Lett.* **2007**, *448*, 88.
- (24) Tzeli, D.; Theodorakopoulos, G.; Petsalakis, I. D. *Frontiers in Quantum Systems in Chemistry and Physics - PTCP. Proceedings of the QCSP-XII*, 2008; Wilson, S.; Grout, P. J.; Maruani, J.; Delgado-Barrio, G.; Piecuch, P., Eds.; Springer Science; 2008, Vol. 18, p 341.
- (25) Harikumar, K. R.; Petsalakis, I. D.; Polanyi, J. C.; Theodorakopoulos, G. *Surf. Sci.* **2004**, *572*, 162.
- (26) Takayanagi, K.; Tanishiro, Y.; Takahashi, M.; Takahashi, S. *J. Vac. Sci. Technol., A* **1985**, *3*, 1502.
- (27) Tong, S. Y.; Huang, H.; Wei, C. M. *J. Vac. Sci. Technol., A* **1988**, *6*, 615.
- (28) Becke, A. D. *J. Chem. Phys.* **1993**, *98*, 1372.
- (29) Lee, C.; Yang, W.; Parr, R. G. *Phys. Rev. B* **1988**, *37*, 785.
- (30) Godbout, N.; Salahub, D. R.; Andzelm, J.; Wimmer, E. *Can. J. Chem.* **1992**, *70*, 560.
- (31) Hay, P. J.; Wadt, W. R. *J. Chem. Phys.* **1985**, *82*, 299.
- (32) Boys, S. F.; Bernardi, F. *Mol. Phys.* **1970**, *19*, 553.
- (33) Tzeli, D.; Mavridis, A.; Xantheas, S. *J. Phys. Chem. A* **2002**, *106*, 11327.
- (34) Tzeli, D.; Tsekouras, A. A. *J. Chem. Phys.* **2008**, *128*, 144103.
- (35) Frisch, M. J.; Trucks, G. W.; Schlegel, H. B.; Scuseria, G. E.; Robb, M. A.; Cheeseman, J. R.; Montgomery, J. A., Jr.; Vreven, T.; Kudin, K. N.; Burant, J. C.; Millam, J. M.; Iyengar, S. S.; Tomasi, J.; Barone, V.; Mennucci, B.; Cossi, M.; Scalmani, G.; Rega, N.; Petersson, G. A.; Nakatsuji, H.; Hada, M.; Ehara, M.; Toyota, K.; Fukuda, R.; Hasegawa, J.; Ishida, M.; Nakajima, T.; Honda, Y.; Kitao, O.; Nakai, H.; Klene, M.; Li, X.; Knox, J. E.; Hratchian, H. P.; Cross, J. B.; Adamo, C.; Jaramillo, J.; Gomperts, R.; Stratmann, R. E.; Yazyev, O.; Austin, A. J.; Cammi, R.; Pomelli, C.; Ochterski, J. W.; Ayala, P. Y.; Morokuma, K.; Voth, G. A.; Salvador, P.; Dannenberg, J. J.; Zakrzewski, V. G.; Dapprich, S.; Daniels, A. D.; Strain, M. C.; Farkas, O.; Malick, D. K.; Rabuck, A. D.; Raghavachari, K.; Foresman, J. B.; Ortiz, J. V.; Cui, Q.; Baboul, A. G.; Clifford, S.; Cioslowski, J.; Stefanov, B. B.; Liu, G.; Liashenko, A.; Piskorz, P.; Komaromi, I.; Martin, R. L.; Fox, D. J.; Keith, T.; Al-Laham, M. A.; Peng, C. Y.; Nanayakkara, A.; Challacombe, M.; Gill, P. M. W.; Johnson, B.; Chen, W.; Wong, M. W.; Gonzalez, C.; Pople, J. A. *Gaussian 03*, revision C.02; Gaussian, Inc.: Wallingford, CT, 2004.
- (36) Koch, W.; Holthausen, M. C. *A Chemist's Guide to Density Functional Theory*, 2nd ed.; Wiley-VCH: New York, 2001.
- (37) Kalemoss, A.; Dunning, T. H., Jr.; Mavridis, A. *J. Chem. Phys.* **2004**, *120*, 1813.
- (38) Bredhol, H.; Dubois, I.; Houbrechts, Y.; Nzohabonayo, P. *J. Mol. Spectrosc.* **1985**, *112*, 430.
- (39) De Maria, G.; Malaspina, L.; Piacente, V. *J. Chem. Phys.* **1972**, *56*, 1978.
- (40) Lorenz, M.; Agreiter, J.; Smith, A. M.; Bondybey, V. E. *J. Chem. Phys.* **1996**, *104*, 3143.
- (41) Kalemoss, A.; Mavridis, A. *J. Phys. Chem. A* **2007**, *111*, 11227.
- (42) Ebben, M.; ter Meulen, J. *J. Chem. Phys. Lett.* **1991**, *177*, 229.
- (43) Chase, M. W. *NIST-JANAF Thermochemical Tables*, J. Phys. Chem. Ref. Data, Monograph 9, 4th ed.; ACS, AIP, NSRDS: Gaithersburg, MD, 1998.
- (44) Demović, L.; Černušák, I.; Theodorakopoulos, G.; Petsalakis, I. D.; Urban, M. *J. Chem. Phys. Lett.* **2007**, *447*, 215.
- (45) Boldyrev, A. I.; Simons, J. *J. Phys. Chem.* **1993**, *97*, 1526.
- (46) Huber, K. P.; Herzberg, G. *Molecular Spectra and Molecular Structure Constants of Diatomic Molecules*; van Nostrand Reinhold: New York, 1979.
- (47) Ornellas, F. R.; Iwata, S. *Chem. Phys.* **1998**, *232*, 95.
- (48) Tzeli, D.; Petsalakis, I. D.; Theodorakopoulos, G. To be submitted.
- (49) McLean, A. D.; Liu, B.; Chandler, G. S. *J. Chem. Phys.* **1992**, *97*, 8459.
- (50) Saito, P. S.; Yasuki, E.; Hirota, E. *J. Chem. Phys.* **1983**, *78*, 6447.